Controlled Microchannelling in Dense Collagen Scaffolds by Soluble Phosphate Glass Fibers

Showan N. Nazhat,*,†,‡ Ensanya A. Abou Neel,† Asmeret Kidane,† Ifty Ahmed,† Chris Hope,§ Matt Kershaw,|| Peter D. Lee,|| Eleanor Stride,⊥ Nader Saffari,⊥ Jonathan C. Knowles,† and Robert A. Brown△

Division of Biomaterials and Tissue Engineering and Division of Microbial Diseases, UCL Eastman Dental Institute, 256 Gray's Inn Road, London, WC1X 8LD, United Kingdom, Department of Materials, Imperial College London, Prince Consort Road, London, SW7 2AZ, United Kingdom, UCL Department of Mechanical Engineering, Torrington Place, London, WC1E 7JE, United Kingdom, and UCL Tissue Regeneration and Engineering Centre, Institute of Orthopaedics, London, HA7 4LP, United Kingdom

Received July 21, 2006; Revised Manuscript Received November 8, 2006

A problem with tissue engineering scaffolds is maintaining seeded cell viability and function due to limitations of oxygen and nutrient transfer. An approach to maintain suitable oxygen concentrations throughout the scaffold would be to controllably incorporate microchannelling within these scaffolds. This study investigated the incorporation of unidirectionally aligned soluble phosphate based glass fibers (PGF) into dense collagen scaffolds. PGF are degradable, and their degradation can be controlled through their chemistry and dimensions. Plastic compression was used to produce composite scaffolds at three different weight percentage while maintaining greater than 80% resident cell viability. PGF-collagen scaffold composition was quantified through thermogravimetric analysis as well as being morphologically and mechanically characterized. PGF degradation was measured through ion chromatography, and channel formation was verified with ultrasound imaging and SEM. The free movement of coated microbubble agents confirmed the channels to be continuous in nature and of 30−40 μm diameter. These microchannels in dense native collagen matrices could play an important role in hypoxia/perfusion limitations and also in the transportation of nutrients and potentially forming blood vessels through dense implants.

Introduction

In the last two decades, tissue engineering has offered a new option for the repair or augmentation of damaged or lost tissues. A reconstituted type I collagen gel is one of the most commonly used naturally based scaffolds in tissue engineering.[1] Under physiological conditions in vitro, the monomers pack into randomly orientated nanosized fibrils to form a loose lattice within an excess of fluid (>99%).[2−4] The liquid content is a result of the casting rather than any inherent swelling property of the collagen. While collagen gels are biologically excellent starting points for scaffold materials, they suffer from a lack of structure and weak mechanical properties. Conventional methods of improving the mechanical properties of these gels have relied either on cell remodeling involving bioreactors, which are time-consuming (often taking weeks),[2,5−7] or chemical cross-linking, which could compromise degradation and biological function.[8]

We recently reported a rapid cell-independent process of producing tissue analogous implants that relies on the removal of fluid from these hyper-hydrated gels through controlled unconfined plastic compression (PC).[9] PC has been shown to produce, in minutes, collagen scaffolds that are dense, mechanically strong, and have controllable meso-scale features (<10 μm scale). Critically, this is achieved independently of cell action while incorporating viable cells. This presents a potentially ideal mechanism for controlling the matrix and cell density, mechanical properties of resultant constructs, as well as the processing of heterogeneous materials that can be sutured in vivo and therefore is potentially suitable for individualized bedside applications.

A potential drawback of the increase in collagen density within compacted gels is the decrease in mass transfer of nutrients leading to hypoxia and damage to deeper cell layers. One way to maintain suitable oxygen concentrations throughout the scaffold would be to controllably incorporate microchannelling within these matrices. These channels would in turn provide means of assisting cell perfusion and potentially vascularization once implanted. To achieve this, we report here the application of PC for the production of dense collagen scaffolds incorporating unidirectionally aligned phosphate glass fibers (PGF). PGF are degradable, and their degradation can range from minutes to years depending on their chemistry.[10−11] Their biocompatibility has also been demonstrated with a number of cell types[10−14] (e.g., osteoblasts, chondrocytes, and tendon fibroblasts). They have also demonstrated myotube formation for skeletal muscle tissue engineering.[13,14] The use of phosphate glass particulates as reinforcing agents and eventually porogens through their degradation in synthetic biodegradable composites has been carried out in poly caprolactone[15,16] and lactide[17,18] matrices developed for drug delivery and tissue engineering scaffolds. However, the use of PGF as channelling devices has not been demonstrated previously.

* Corresponding author. Tel.: 001-514-398-5524. Fax: 001-514-398-4492. E-mail: showan.nazhat@mcgill.ca.

† Division of Biomaterials and Tissue Engineering, UCL Eastman Dental Institute.

‡ Current address: Department of Mining, Metals, and Materials Engineering, McGill University, 3610 University Street Montreal, Quebec, H3A 2B2, Canada.

§ Division of Microbial Diseases, UCL Eastman Dental Institute.

|| Imperial College London.

⊥ UCL Department of Mechanical Engineering.

△ UCL Tissue Regeneration and Engineering Centre.

10.1021/bm060715f CCC: $37.00
Published on Web 12/24/2006

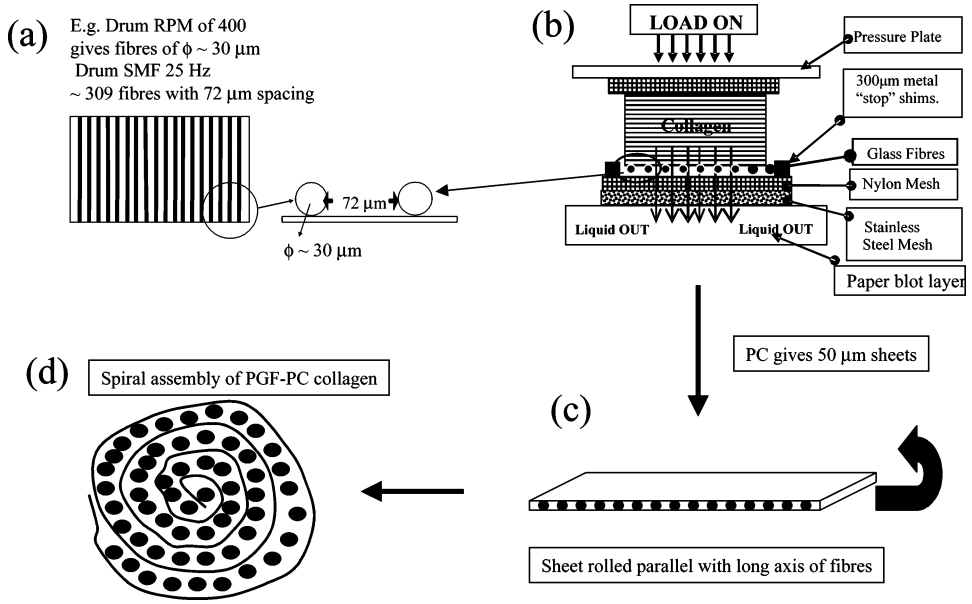

Figure 1. Schematic overview of a routine method used for production of PGF-collagen scaffolds. (a) Aligned fibers at, for example, a drum rotational speed in revolutions per minute (rpm) of 400 m min^{-1} and a stepper motor frequency (SMF) of 25 Hz showing the theoretical fiber number and spacing between two adjacent fibers. (b) Standard compressive load was 1.5 kN m^{-2} for 5 min at 37 °C giving PGF-collagen sheets (~50 μm thick). (c) Sheets rolled along their short axis. (d) PGF-Collagen spiral constructs (2 ± 0.2 mm diameter).

Experimental Procedures

Formation of PGF-PC Collagen Scaffolds. Figure 1 shows schematically the method applied to incorporate unidirectionally aligned PGF into compacted collagen. The PGF formulations used for this study were the more durable quaternary composition (in mol fraction) 0.5-$(P_2O_5)-0.3(CaO)-0.17(Na_2O)-0.03(Fe_2O_3)$ to demonstrate preparation of the composite scaffolds and the more degradable ternary composition $0.5(P_2O_5)-0.25(CaO)-0.25(Na_2O)$ to demonstrate microchannelling. Continuous PGF were produced onto a drum from the melt using a custom-made fiber rig as previously described.[11,13,14] Factors such as the drum rotational speed in revolutions per minute (rpm) and the stepper motor frequency (SMF) control the fiber diameter, fiber to fiber spacing, and PGF number in the scaffold. PGF of the range of 30−40 μm diameter were used in this study.

Reconstituted rat tail type I collagen gels (First Link) were prepared as previously described.[9] After neutralization with NaOH, 2 mL of collagen solution was pipetted into a rectangular mold (Delrin polymer, ~33 mm × 13 mm × 4 mm) and was allowed to set/stabilize for 30 min at 37 °C. After removal from the mold, the scaffold was routinely compacted by a combination of compression and capillary action using layers of meshes and tissue. A compressive stress of 1.5 kN m^{-2} was applied for 5 min at 37 °C, which was used as a standard. Collagen sheets of approximately 50 μm thickness were produced through the expulsion of >97 wt % fluid. For the production of PGF-collagen, the unidirectionally pre-aligned fibers were placed on a glass slide that formed the base of the mold before collagen setting and compaction. The compressed sheets were then rolled along their short axis (parallel to the long axis of the glass fibers) to give a spirally assembled scaffold (of approximate length of 13 mm and diameter of 2 ± 0.2 mm). Three sets of spirally assembled scaffolds were produced, each incorporating the different amounts of PGF as dictated by the different drum SMFs.

Morphological Characterizations. Scanning electron microscopy (SEM) and X-ray microtomography (XMT) were used for morphological characterizations. Samples for SEM were fixed in 4% paraformaldehyde in 0.1 M sodium cacodylate buffer overnight. These were washed in distilled water for 10 min, followed by soaking for 1 h in 1% tannic acid (w/v) in 0.05 M sodium cacodylate for further fixation or stabilization of collagen fibrils.[19,20] The samples were then dehydrated in a graded ethanol series to hexamethyldisilazane (HMDS) for further drying. The dried samples were mounted on aluminum stubs and then sputter coated with gold palladium alloy before being examined under a scanning electron microscope (JOEL JSM-5500LV) with an accelerating voltage of 15 kV.

Spiral construct samples for XMT were cut to approximately 5 mm in length and inserted vertically into polymer specimen holders designed for minimal X-ray attenuation and kept in standard growth medium during analysis. Prepared specimens were analyzed using X-ray microtomography apparatus (Phoenix X-ray V|tome|Xs) using X-ray parameters of 80 kV and 80 μA. Projections were acquired at angular separations of 0.5°, resulting in a total of 720 transmission images. The magnification of the transmission images was approximately 115, giving a voxel resolution in the reconstructed images of 3.5 ± 0.1 μm. Reconstruction was performed using the commercially available Sixtos software package.

Quantification of Composition and Mechanical Properties. Thermo-gravimetric analysis (TGA) was used to quantify scaffold components. This was determined using a Setaram Differential Thermal Analyzer (DTA/TGA). Sample mass loss was observed between 20 and 270 °C at a rate of 20 °C min^{-1}. Greater than five repeat specimens of 110 ± 5 mg were tested, and a blank baseline run was subtracted from the sample data.

Tensile mechanical tests were carried out on compacted spiral constructs using a Pyris run Perkin-Elmer DMA-7e (Perkin-Elmer Instruments). The diameter of each sample was measured with a travelling microscope, giving an average diameter of 2 ± 0.2 mm. The samples were clamped at the ends using a 2 mm strip of 165 μm thick steel mesh reinforced by cyanoacrylate adhesive to facilitate gripping during testing. The tests were conducted at room temperature, and constant sample hydration was maintained by the application of Earl's Balanced Salt Solution. The initial applied load was 1 mN, and the specimen was tested until failure at a loading rate of 200 mN min^{-1}. From the stress−strain curve, the average modulus of elasticity, ultimate tensile strength, and strain to break were calculated from seven to 10 repeat specimens.

Cellular Scaffolds. Determination of cell viability was carried out up to 24 h to assess the effect of processing and fiber inclusion on cells. Cellular constructs were produced by adding human oral fibroblasts (HOFs) with the collagen solution immediately after neutralization at a density of 3.3 × 10^5 cells/mL of collagen before setting and compaction. The seeded constructs were placed in 60 mm

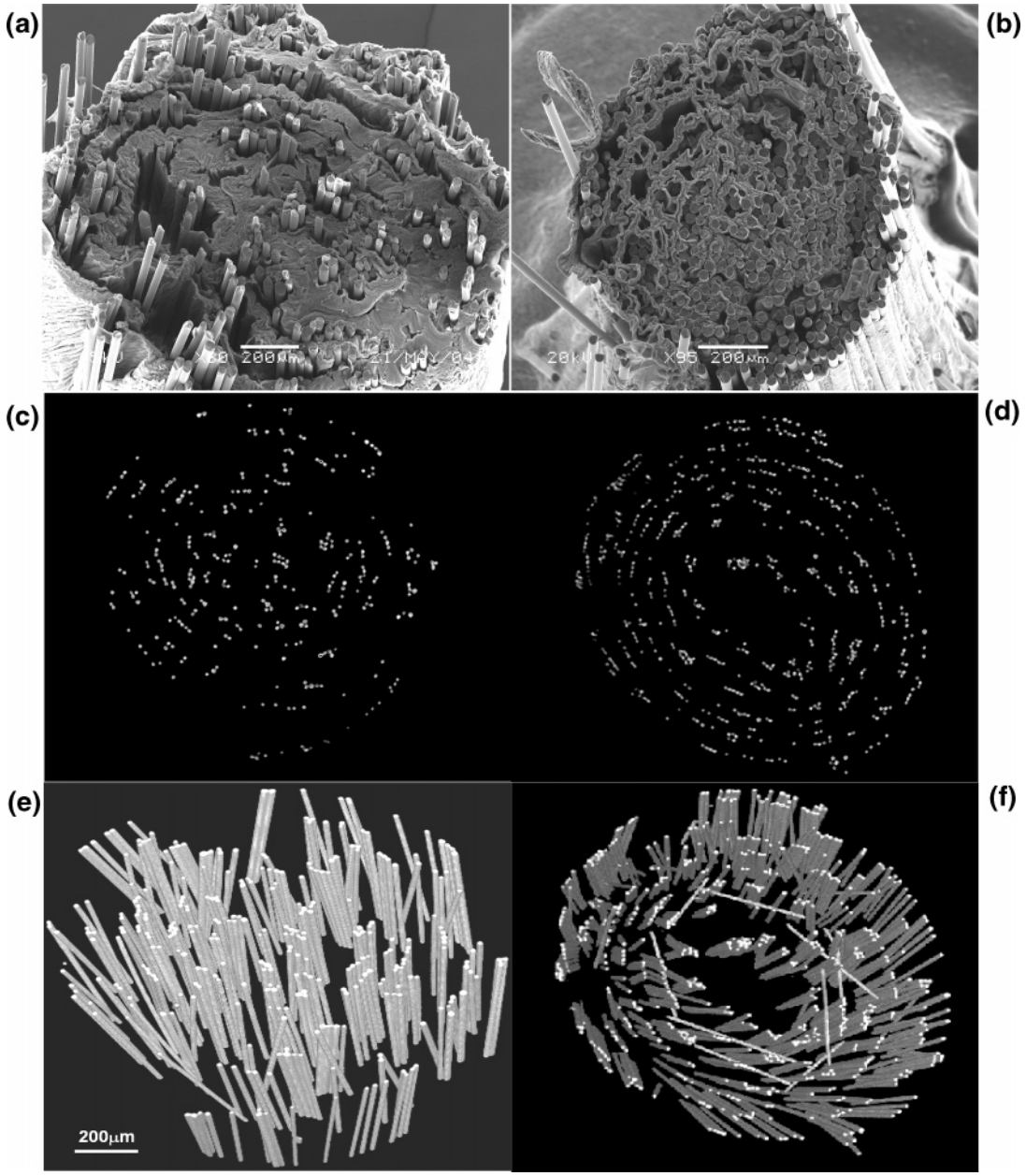

Figure 2. Morphological characterizations of PGF-collagen scaffolds. (a) SEM of cross-sectional PGF-collagen spiral constructs with PGF generated at 25 Hz SMF and (b) with PGF generated at 12.5 Hz SMF. (c) Cross-sectional XMT image of PGF-collagen spiral constructs with PGF generated at 25 Hz SMF and (d) with PGF generated at 12.5 Hz SMF. (e) Three-dimensional XMT image of PGF-collagen spiral constructs with PGF generated at 25 Hz SMF and (f) with PGF generated at 12.5 Hz SMF.

vculture dishes with 10 mL of standard growth medium [Dulbecco's Modified Eagle's Medium, 10% foetal calf serum (FCS), 1% L-glutamine (L-Glut), 1% penicillin (100 IU/mL)/streptomycin (100 μg/mL), and 1% amphotericin B] and incubated in a humid atmosphere of 5% CO_2 at 37 °C for up to 1 and 24 h. Constructs were incubated for 1 h in a standard growth medium containing 1 μL/mL calcein AM, to stain the live cells, and propidium iodide, to stain the dead cells. Live cells cleaved membrane-permeant calcein AM to yield cytoplasmic green fluorescence; membrane-impermeant propidium iodide labels nucleic acids of membrane compromised cells with red fluorescence. Constructs were washed with dye-free PBS buffer after loading for 5 min. The assessment of cell viability in three dimensions was performed using confocal microscopy (Bio-Rad). In a typical scan, the sample was placed in a 60 mm culture dish, and sections of the sample were scanned using a 20× lens. The region of interest was 600 μm × 600 μm, the $x-y$ dimension, and the images were collected at 2 μm intervals through a 50−70 μm thickness of the compressed sheet and 400 μm (nominal thickness) of gel in the z-dimension (z-stacks) using Laser Sharp 2000 software. Excitation wavelengths for the fluorescent dyes for live and dead cells were provided at 488 nm from an argon laser and 543 nm from a green/HeNe laser, respectively. Projection images were created by superimposing the z-stack images that were captured throughout the construct thickness using ImageJ software (National Institute of Health). Average % cell viability was calculated from five randomly chosen areas from each image.

Fiber Degradation. Ion release measurements through ion chromatography were carried out to determine PGF degradation. Cation release profiles of Na^+ and Ca^{2+} ions were investigated using a Dionex ICS− 1000. A 30 mM methanesulfonic acid (MSA, BDH) solution was used as the eluent. Cations were eluted using a 4 mm × 250 mm IonPac CS12A separator column, in combination with a 4 mm CSRS suppressor. Sodium chloride (Sigma) and calcium chloride (BDH) were used as standard reagents. A 100 ppm mixed (sodium and calcium) stock solution was prepared, from which serially diluted 50, 25, 10, and 1 ppm standard solutions were made.

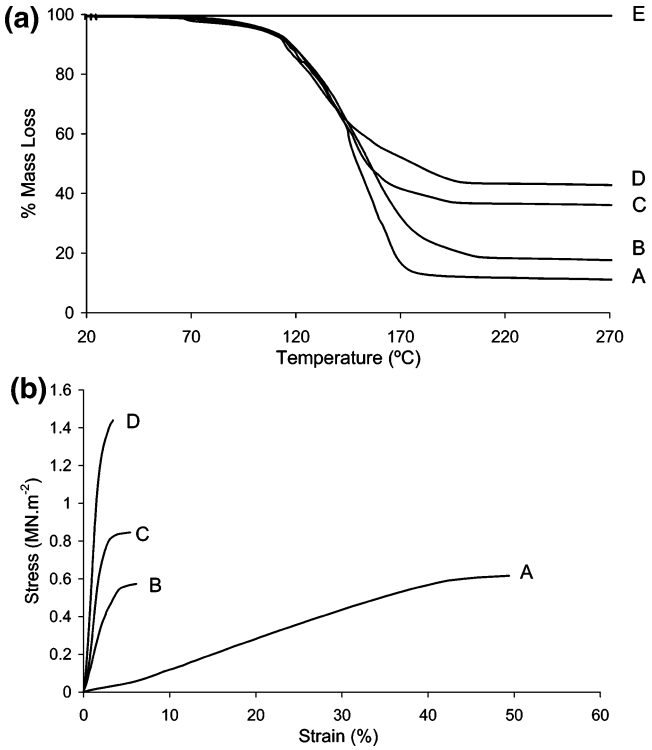

Figure 3. Quantification and mechanical characterization of PGF-collagen scaffolds (a) TGA thermograms of (A) collagen spiral and (B) 8 wt %, (C) 21 wt %, and (D) 30 wt % PGF-collagen and (E) PGF. (b) Stress−strain curves obtained from quasi-static tensile testing (A) collagen and (B) 8 wt %, (C) 21 wt %, and (D) 30 wt % PGF-collagen spiral constructs.

Phosphate anions (PO_4^{3-}, $P_2O_7^{4-}$, $P_3O_9^{3-}$, and $P_3O_{10}^{5-}$) were quantified using a Dionex ICS-2500 system (Dionex). This consisted of a gradient pump with a 25 μL sample loop, a 4 mm × 250 mm IonPac AS16 anion-exchange column along with a Dionex ASRS (anion self-regenerating suppressor) used at 223 mA. A Dionex EG50 eluent generator equipped with a KOH cartridge was used in conjunction with the ASRS. The EG50 eluent generator system electrolytically produced high-purity KOH using deionized water as the carrier stream to the point of use. The sample run time was set for 20 min. Sodium phosphate tribasic (Na_3PO_4), trisodium trimetaphosphate ($Na_3P_3O_9$), pentasodium tripolyphosphate ($Na_5P_3O_{10}$) (all from Sigma-Aldrich), and tetra-sodium pyrophosphate ($Na_4P_2O_7$) (BDH) were used as standard reagents. A 100 ppm working solution containing all four reagents was made, from which serially diluted 50, 25, 10, and 1 ppm standard solutions were prepared.[21−22] The Chromeleon software package was used for data analysis for both systems.

Ultrasound Imaging. Post PGF degraded scaffolds were immersed in a bath containing distilled water at room temperature, and a length of Tygon tubing (inner diameter 2.4 mm) was attached to each end, using putty to ensure a tight seal. Distilled water was forced through the scaffold by applying gentle pressure to a 1 mL syringe connected to one length of the tubing. The second length of tubing was fed out into a beaker. An ultrasound C-Scan of the scaffold was performed with a step size of 35 μm using a 50 MHz focused transducer (V3330, Panametrics) activated by a pulser-receiver (5601T, Panametrics). The signals from the transducer were captured using a digital oscilloscope (LeCroy 9310M dual 300 MHz) connected to a PC. For each point in the scan, an A-scan trace was also captured to produce a three-dimensional image of the scaffold. Images were produced in Matlab (version 6.0, release 12.1, The Mathworks). This procedure was repeated, substituting a suspension of coated microbubbles (Expancel, Casco Products AB) for the distilled water that was passed through the sample. The suspension concentration was approximately 10^9 microbubbles/mL, and the mean microbubble diameter was 15 μm. A second set of scans was then made of the control scaffold. In all cases, the flow rate through the scaffold was much lower than the scanning rate.

Table 1. Summary of Average Mass Loss % of PGF-Collagen with Three Different Amounts of PGF and Its Individual Components from TGA and Scaffold Components (in wt %) Calculated at 200 °C

	wt % at 200 °C		
materials	fluid	collagen	PGF
Collagen	85.4 ± 2.2	14.6 ± 2.2	
low PGF-collagen (SMF 50 Hz)	77.0 ± 6.2	14.6 ± 2.2	8.4 ± 6.2
medium PGF-collagen (SMF 25 Hz)	55.3 ± 6.3	14.6 ± 2.2	20.7 ± 2.4
high PGF-collagen (SMF 12.5 Hz)	64.7 ± 2.4	14.6 ± 2.2	30.1 ± 6.3

Table 2. Summary of Mechanical Properties in Terms of Modulus, Tensile Strength, and Strain at Failure, Presented as Mean ± Standard Deviation of PGF-Collagen with Three Different PGF Contents and PC Collagen as a Control

materials	modulus (MN m^{-2})	tensile strength (MN m^{-2})	break strain (%)
Collagen	1.3 ± 0.3	0.6 ± 0.1	55.0 ± 13.8
8 wt % PGF-collagen	7.8 ± 3.1	0.5 ± 0.2	7.7 ± 3.5
21 wt % PGF-collagen	33.4 ± 10.2	1.27 ± 0.4	6.7 ± 1.8
30 wt % PGF-collagen	164.9 ± 59.6	2.3 ± 0.6	3.4 ± 1.2

Table 3. Percentage Cell Viability in Immediately and 24 h Seeded Collagen Sheets and Spiral Constructs as Compared to Noncompressed Gel Control

	cell viability (%)	
samples	immediate	24 h
noncompressed collagen	88.3 ± 8.3	85.9 ± 5.2
collagen sheet	86.5 ± 7.7	100[a]
collagen spiral		77.4 ± 7.7
8 wt % PGF-collagen sheet	87.4 ± 9.5	98.4 ± 1.5
8 wt % PGF-collagen spiral		83.8 ± 4.4
21 wt % PGF-collagen sheet	80.4 ± 2.8	96 ± 2.3
21 wt % PGF-collagen spiral		75.3 ± 8.4
30 wt % PGF-collagen sheet	80 ± 5.3	100[a]
30 wt % PGF-collagen spiral		79.7 ± 0.4

[a] No dead cells were detected in either PC-collagen only or 30 wt % PGF-collagen sheets, probably due to the high cell density.

Results and Discussion

Scaffold Morphology. In this study, PGF were produced from the melt, and by adjusting the rig parameters, control can be exerted on the fiber diameter (which can range from 10 to 50 μm), spacing, and number within scaffolds. A standard PC technique was applied to produce PGF−-collagen sheets in the range of 50 μm thickness. These sheets were then rolled parallel to the long axes of the fibers to form three-dimensional spiral constructs. Typical SEM images of the cross-section of the PGF-collagen spirals are shown in Figure 2a,b, which show the effect of changing the rig SMF from 25 to 12.5 Hz and thereby increasing the number of fibers. Generally, the fibers were well-distributed throughout the dense collagen scaffolds. Figure 2c−f shows cross-sectional and three-dimensional views of spirals produced through similar SMFs, as obtained using X-ray microtomography (XMT). The contrast in these micrographs

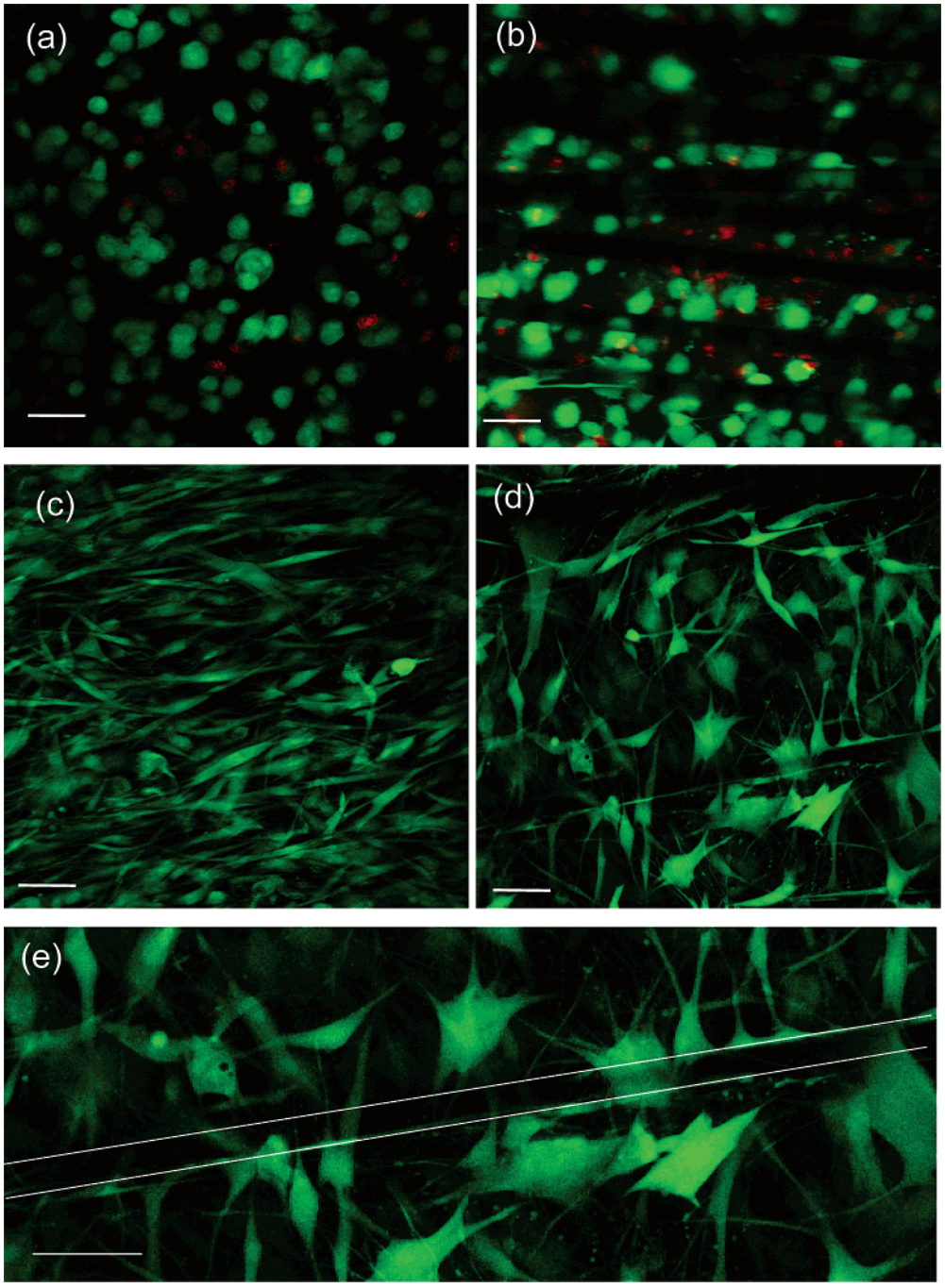

Figure 4. Confocal laser scanning micrographs of HOFs within PC-collagen and PGF-PC collagen. (a) Immediately within PC-collagen, (b) within 21 wt % PGF-collagen sheets, (c) after 24 h culture within PC-collagen, (d) in 21 wt % PGF-collagen sheets, (e) closer view of HOFs seeded in 21 wt % PGF-collagen sheet after 24 h demonstrating that the attachment of cells showed no preference to either collagen or PGF (dashed white lines indicating the edges of a glass fiber). Live cells are green, and dead cells are red. Scale bar is 50 μm.

was manipulated to render the collagen in the specimen transparent, allowing quantification of PGF. The number of PGF in the scaffolds from the cross-sectional XMT images was comparable to calculated numbers (i.e., within 5% error). The micrographs generated using XMT provided an excellent illustration of the degree of alignment of the PGF within the scaffold, showing that the fibers are generally well-aligned with respect to each other, and demonstrated clear zones between separate sheets in the spirally assembled constructs. As in the SEM images, the clustering and misalignment of some PGF were also seen, which could be attributed to several factors such as the open air environment in which the fibers were pulled, the compression method, and the handmade processing of the scaffolds. This, in turn, will have a bearing on the mechanical performance of the scaffolds.

Scaffold Composition and Mechanical Properties. The quantification of the three main phases in these scaffolds (fluid, collagen, and glass fibers) was carried out using thermogravimetric analysis. Figure 3a shows the TGA thermograms of PGF, collagen, and PGF-collagen spirals with three weight percentages generated by adjusting the fiber rig parameters. Between 100 and 180 °C, both collagen and PGF-collagen scaffolds showed significant mass loss due to water loss, whereas the overall trend for the PGF alone showed a negligible mass loss over the same temperature range. The wt % of the various components was calculated at 200 °C as water was

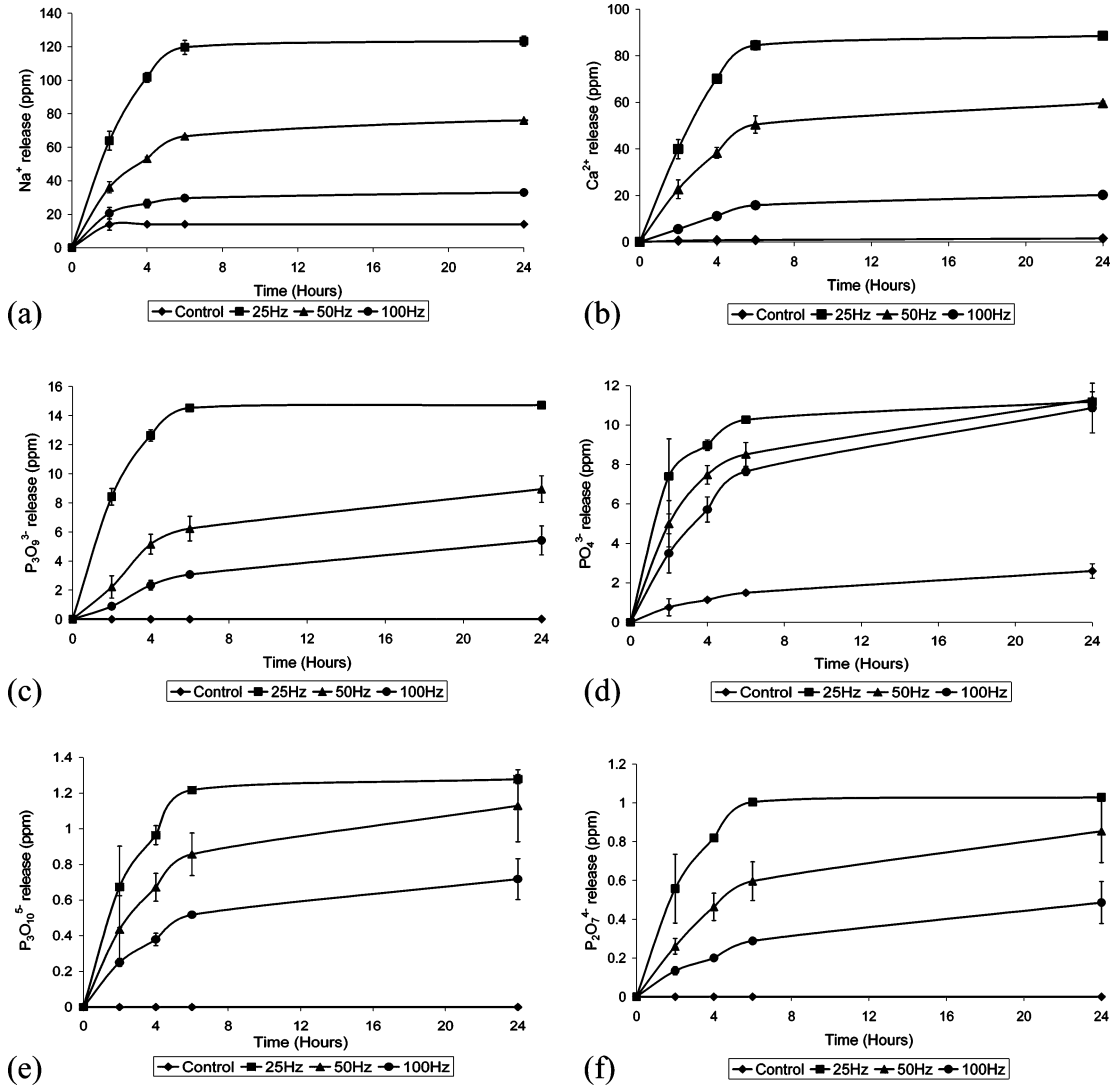

Figure 5. Ion release measurements through degradation of PGF in PGF-collagen spirals generated from a drum rotational speed of 300 m min^{-1} giving diameters of 37.6 ± 7.5 μm and SMF of 100, 50, and 25 Hz giving the corresponding number of fibers 60, 120, and 232, respectively. Cation release measurements (a) Na^+, (b) Ca^{2+}, and anion release measurements (c) $P_3O_9^{3-}$, (d) PO_4^{3-}, (e) $P_3O_{10}^{5-}$, and (f) $P_2O_7^{4-}$ as measured using ion chromatography. Release was linear up to 6 h in deionized water.

completely eliminated from the scaffold, which has also been identified elsewhere.[23−26] The three main components present within the scaffolds are given in Table 1. Tensile mechanical tests were carried out to investigate the effect of incorporating PGF into the dense collagen scaffolds. Figure 3b shows typical stress−strain curves for three different weight percentages of PGF-collagen spirals (quantified through TGA) and compared to collagen only scaffolds. The tensile behavior of fibrillar collagen consists of three main regions: toe region, linear region, and a failure region. The compliant toe region is associated with the nanosized fibrillar realignment in the axis of loading. The linear region is the resistance to loading leading to the failure region. The mechanical behavior of the scaffolds significantly changed with composite composition since in this mode of analysis the glass fibers would be the main load bearing component. This indicated that these scaffolds could be produced for a specific end application. Table 2 gives a summary of the mechanical properties of the spiral assembled collagen only and PGF-collagen. There was a significant ($P < 0.05$) increase in strength and modulus with the incorporation of PGF and a significantly lower elongation to break.

Cell Viability. Figure 4a−e shows the morphology of human oral fibroblast (HOF) seeded dense collagen constructs with and without PGF incorporation at 21 wt %. Cells were seeded between gel neutralization and compaction. Immediately after compaction in the composite constructs, regions of focused cell death were present near the fibers possibly due to their high stiffness in combination with the compressive and/or shear forces experienced due to the rapid removal of fluid. Cell processes were only visible within the noncompressed gels (data not presented). This contrasted with the rounded cell morphologies observed in the dense constructs with or without PGF (Figure 4a,b), suggesting that cell movements were much slower in the dense constructs than through initially hyper-hydrated gels. Not surprisingly, the cells were denser in the compacted constructs than in noncompressed gels in parallel with the increased collagen density since PC fabrication results in a >97 wt % decrease in fluid loss accompanied by ~99 fold in height reduction. After 24 h, the cells took on a tightly packed spindle shaped appearance in three-dimensions in the compacted collagen (Figure 4c) and PGF-collagen (Figure 4d) sheets. Figure 4e shows a closeup view of HOF cells aligned along a glass fiber after 24 h. Loss of cell viability of the resident fibroblasts

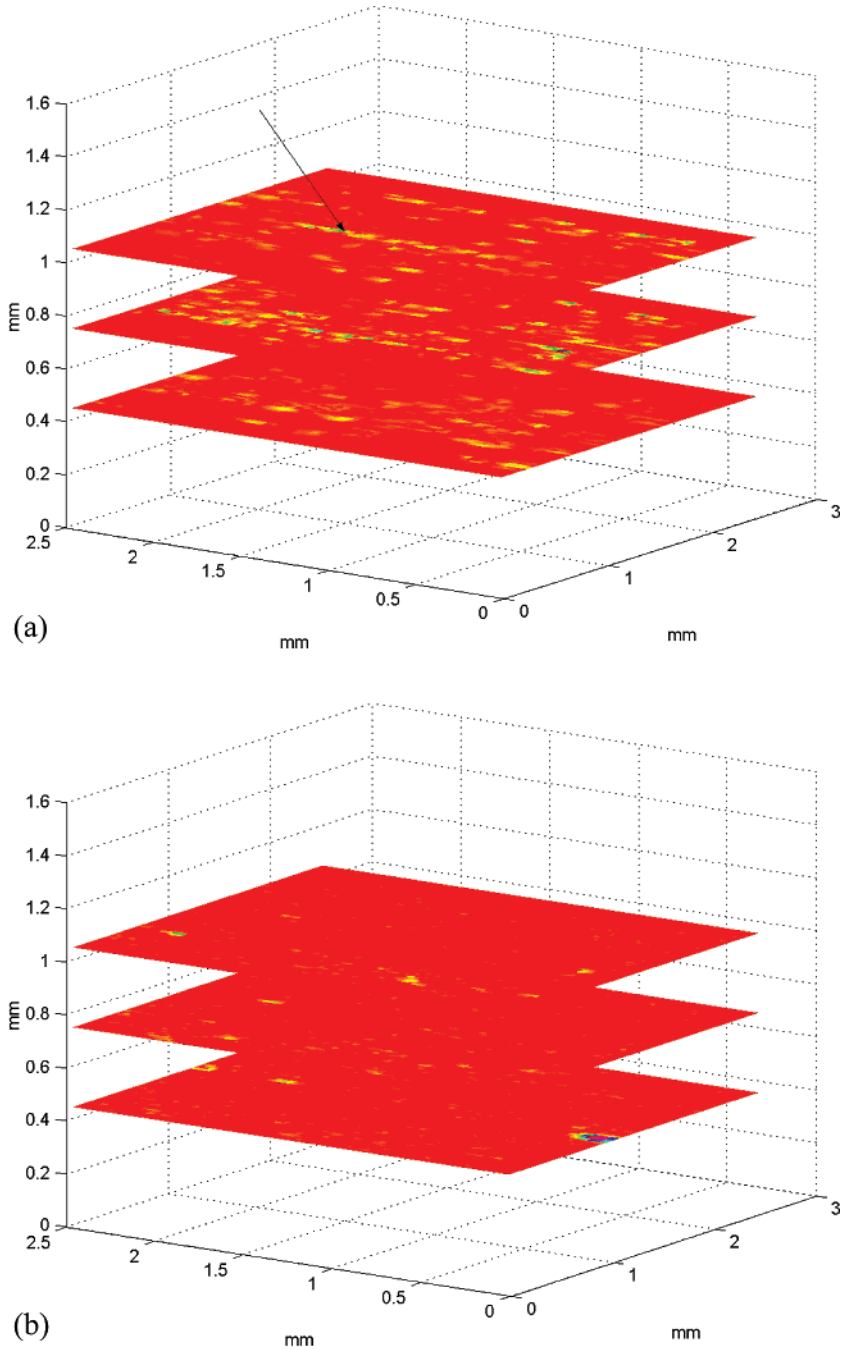

Figure 6. Confirmation of channel formation. Three-dimensional ultrasound image showing (a) the passage of coated microbubbles as indicated by the arrow through a channelled collagen scaffold (green and yellow tracks; scale: 35 μm per pixel) and compared to (b) the collagen alone spiral showing no channelling.

was at its maximum only 20% across all types of constructs (Table 3). There was no significant difference ($P > 0.05$) in the immediate % cell viability between noncompressed collagen control, PC collagen, and PGF-PC collagen sheets. After 24 h, while there was a significant increase in cell viability in the dense sheets, there was also a significant reduction within the spiral constructs. This difference in the viable cell number between spirals and sheets may be due to increased perfusion limitations as a consequence of the size of spirals (i.e., the diffusion distance (2 mm diameter spirals as compared to approximately 50 μm thick sheets)). Perfusion limitations may be overcome within these dense spirals by the degradation of the PGF, thus providing channelling for oxygen, nutrients, and waste products.

Monitoring of Fiber Degradation. The degradation of the fibers within the scaffolds was demonstrated by ion chromatography. Figure 5a−f shows the release of Na^+ and Ca^{2+} cations and the phosphate anions, which were composed of cyclic trimetaphosphate ($P_3O_9^{3-}$), orthophosphate (PO_4^{3-}), pyrophosphate ($P_2O_7^{4-}$), and tripolyphosphate ($P_3O_{10}^{5-}$). The release profile of these ions through the degradation of the fibers was linear within the first 6 h, which was in line with weight loss, demonstrating the controlled degradation of these glass fibers.[11,27] The rate of ion release was clearly linked to the amount of fibers present within the scaffolds as dictated by the rig SMF. Generally, the degradation behavior of PGF is affected by the glass chemistry and fiber size. The rate of release of the ions would decrease with increasing fiber diameters and an increase in the ion concentration of the external environment

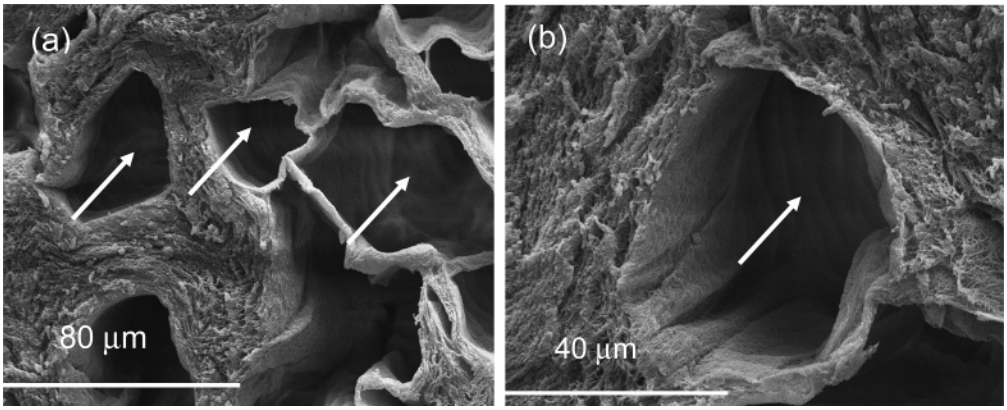

Figure 7. Channel formation via the degradation of PGF in PGF-collagen spirals. (a) SEM image of a cross-section through the collagen scaffold leaving a cluster of channels left as the fibers degraded and (b) SEM image of a closeup of a channel after fiber degradation.

(this study was carried out in deionized water and not simulated body fluids or culture medium).

Characterization of Microchannelling. Microchannelling within the collagen scaffolds was confirmed by ultrasound imaging of through movement of coated microbubble agents. This is routinely used in diagnostic medical imaging to improve the contrast between the vasculature and the surrounding tissue.[28] As shown in Figure 6a, distinct echoes were received from locations throughout the scaffold upon injecting the microbubble suspension. The amplitude of the echoes was far larger than those detected with distilled water in the scaffold, indicating that the microbubbles were flowing freely through the structure. Moreover, each set of echoes was detected from an individual plane, which suggested that the microbubbles were passing through continuous channels and that the size of the channels corresponded to the diameter of PGF (30−40 μm). In contrast, as in Figure 6b, there was no noticeable change in the echoes received from control scaffolds, without PGF, upon injecting the microbubble suspension. Indeed, it was not possible to force either distilled water or the microbubble suspension through the control without increasing the applied pressure considerably. This implied that there were no continuous channels through the control. Figure 7a,b shows SEM images that demonstrate the channel formation post fiber degradation. The size of the channelling was dependent on the original size of the fibers, which can range from 10 to 50 μm, and is ideally sized for mammalian tissue models. In some instances, the size of the channel was greater than the size of a single fiber in line with the presence of fiber clusters. These microchannel formations, while confirming the plastic deformation nature of these dense collagen matrices, could play an important role in hypoxia/perfusion limitations and also in the long distance transportation of cells,[29] nutrients, and potentially blood vessels through dense implants.

Conclusion

This study has demonstrated that the method of rapidly compacting collagen gels can be employed for the development of three-dimensional scaffolds with PGF for channel formation in implant materials. The PC fabrication process has been demonstrated to be fast, efficient, and versatile in adding a second component to generate more complex structures and maintain greater than 80% cell viability. The process could be scalable to produce multilayered dense sheets incorporating fibers of different orientations, chemistry, and size as well as particulates and short fiber reinforced matrices. The multiple layering would also allow for the possibility of segregating different cell types in co-cultures as an approach for regenerating tissue interface structures, such as the hard−soft tissue enthesis. Initially, the incorporation of phosphate-based fibers into these dense collagen sheets would be an ideal route to control the mechanical properties of the scaffolds to suit an end application. Furthermore, their controlled degradation would introduce means for improving perfusion, cell ingrowth, and hence implant−host integration along with potential for drug delivery systems.

Acknowledgment. The help and advice of Malak Bitar, Mike Wiseman, Aviva Petrie, Nicky Mordan, and the late Mike Kayser are gratefully acknowledged. E.A.A.N.'s project is supported by the Egyptian Government. The U.K. EPSRC and BBSRC for the TIBS funding are also acknowledged.

References and Notes

(1) Wallace, D. G.; Rosenblatt, J. Collagen gel systems for sustained delivery and tissue engineering. *Adv. Drug Delivery Rev.* **2003**, *55*, 1631−1649.
(2) Eastwood, M.; Mudera, V. C.; McGrouther, D. A.; Brown, R. A. Effect of precise mechanical loading on fibroblast populated collagen lattices: Morphological changes. *Cell Motil. Cytoskeleton* **1998**, *40*, 13−21.
(3) Feng, Z.; Yamato, M.; Akutsu, T.; Nakamura, T.; Okano, T.; Umezu, M. Investigation on the mechanical properties of contracted collagen gels as a scaffold for tissue engineering. *Artif. Organs* **2003**, *27*, 84−91.
(4) Krishnan, L.; Weiss, J. A.; Wessman, M. D.; Hoying, J. B. Design and application of a test system for viscoelastic characterization of collagen gels. *Tissue Eng.* **2004**, *10*, 241−252.
(5) Moriyama, T.; Asahina. I.; Ishii, M.; Oda, M.; Ishii, Y.; Enomoto, S. Development of composite cultured oral mucosa utilizing collagen sponge matrix and contracted collagen gel: A preliminary study for clinical application. *Tissue Eng.* **2001**, *7*, 415−427.
(6) Garvin, J.; Qi, B.; Maloney, M.; Banes, A. J. Novel system for engineering bioartificial tendons and application of mechanical load. *Tissue Eng.* **2003**, *9*, 976−979.
(7) Shi, Y.; Vesely, I. Fabrication of mitral valve chordae by directed collagen gel shrinkage. *Tissue Eng.* **2003**, *9*, 1233−1242.
(8) Charulatha, V.; Rajaram, A. Influence of different cross-linking treatments on the physical properties of collagen membranes. *Biomaterials* **2003**, *24*, 759−767.
(9) Brown, R. A.; Wiseman, M.; Chuo, C. B.; Cheema, U.; Nazhat, S. N. Ultrarapid engineering of biomimetic materials and tissues: Fabrication of nano- and microstructures by plastic compression. *Adv. Funct. Mater.* **2005**, *15*, 1762−1770.
(10) Knowles, J. C. Phosphate-based glasses for biomedical applications. *J. Mater. Chem.* **2003**, *13*, 2395−2401.
(11) Abou Neel, E. A.; Ahmed, I.; Blaker, J. J.; Bismarck, A.; Boccaccini, A. R.; Lewis, M. P.; Nazhat, S. N.; Knowles, J. C. Effect of iron on the surface, degradation, and ion release properties of phosphate-based glass fibers. *Acta Biomater.* **2005**, *1*, 553−563.

(12) Bitar, M.; Salih, V.; Mudera, V.; Knowles, J. C.; Lewis, M. Soluble phosphate glasses: In vitro studies using human cells of hard and soft tissue origin. *Biomaterials* **2004**, *25*, 2283−2292.
(13) Ahmed, I.; Collins, C. A.; Lewis, M.; Olsen, I.; Knowles, J. C. Processing, characterization, and biocompatibility of iron−phosphate glass fibers for tissue engineering. *Biomaterials* **2004**, *25*, 3223−3232.
(14) Shah, R.; Sinanan, A. C. M.; Knowles, J. C.; Hunt, N. P.; Lewis, M. P. Craniofacial muscle engineering using a 3-D glass fiber construct. *Biomaterials* **2005**, *26*, 1497−1505.
(15) Prabhakar, R. L.; Brocchini, S.; Knowles, J. C. Effect of glass composition on the degradation properties and ion release characteristics of phosphate glass−polycaprolactone composites. *Biomaterials* **2005**, *26*, 2209−2218.
(16) Kim, H. W.; Lee, E. J.; Jun, I. K.; Kim, H. E.; Knowles, J. C. Degradation and drug release of phosphate glass/polycaprolactone biological composites for hard tissue regeneration. *J. Biomed. Mater. Res.* **2005**, *75*, 34−43.
(17) Navarro, M.; Ginebra, M. P.; Planell, J. A.; Zeppetelli, S.; Ambrosio, L. Development and cell response of a new biodegradable composite scaffold for guided bone regeneration. *J. Mater. Sci.: Mater. Med.* **2004**, *15*, 419−422.
(18) Georgiou, G.; Mathieu, L.; Pioletti, D. P.; Bourban, P-E.; Månson, J.-A. E.; Knowles, J. C.; Nazhat, S. N. Polylactic acid−phosphate glass composite foams as scaffolds for bone tissue engineering. *J. Biomed. Mater. Res.*, DOI: 10.1002/jbm.b.30600.
(19) Simionescu, N.; Simionescu, M. Galloylglucoses of low molecular weight as mordant in electron microscopy. 1. Procedure and evidence for mordanting effect. *J. Cell Biol.* **1976**, *70*, 608−621.
(20) Wollweber, L.; Stracke, R.; Gothe, U. The use of a simple method to avoid cell shrinkage during SEM preparation. *J. Microsc. (Oxford)* **1981**, *121*, 185−189.
(21) Ahmed, I.; Lewis, M. P.; Nazhat, S. N.; Knowles, J. C. Quantification of anion and cation release from a range of ternary phosphate-based glasses with fixed 45 mol% P_2O_5. *J. Biomater. Appl.* **2005**, *20*, 65−80.
(22) Ahmed, I.; Lewis, M. P.; Knowles, J. C. Quantification of anions and cations from ternary phosphate-based glasses with fixed 50 and 55 mol% P_2O_5 using ion chromatography. *Phys. Chem. Glasses* **2005**, *46*, 547−552.
(23) Samouillan, V.; Dandurand-Lods, J.; Lamure, A.; Maurel, E.; Lacabanne, C.; Gerosa, G.; Venturini, A.; Casarotto, D.; Gherardini, L.; Spina, M. Thermal analysis characterization of aortic tissues for cardiac valve bioprostheses. *J. Biomed. Mater. Res.* **1999**, *46*, 531−538.
(24) Samouillan, V.; Dandurand, J.; Lacabanne, C.; Thoma, R. J.; Adam, A.; Moore, M. Comparison of chemical treatments on the chain dynamics and thermal stability of bovine pericardium collagen. *J. Biomed. Mater. Res.* **2003**, *64*, 330−338.
(25) Kumar, T. R.; Shanmugasundaram, N.; Babu, M. Biocompatible collagen scaffolds from a human amniotic membrane: physicochemical and in vitro culture characteristics. *J. Biomater. Sci., Polym. Ed.* **2003**, *14*, 689−706.
(26) Shanmugasundaram, N.; Ravikumar, T.; Babu, M. Comparative physicochemical and in vitro properties of fibrillated collagen scaffolds from different sources. *J. Biomater. Appl.* **2004**, *18*, 247.
(27) Abou Neel, E. A.; Ahmed, I.; Pratten, J.; Nazhat, S. N.; Knowles, J. C. Characterization of antibacterial copper releasing degradable phosphate glass fibers. *Biomaterials* **2005**, *26*, 2247−2254.
(28) Stride, E. N.; Saffari, N. Microbubble ultrasound contrast agent: a review. *J. Engineering Med., Proc. Inst. Mech. Eng.* **2003**, *217*, 429−447.
(29) Ahmed, Z.; Underwood, S.; Brown, R. A. Low concentrations of fibrinogen increase cell migration speed on fibronectin cables. *Cell Motil. Cytoskeleton* **2000**, *46*, 6−16.

BM060715F